Long-term ordering kinetics of the two-dimensional q-state Potts model

Ezequiel E. Ferrero* and Sergio A. Cannas†
Facultad de Matemática, Astronomía y Física, Universidad Nacional de Córdoba, Ciudad Universitaria, 5000 Córdoba, Argentina
(Received 2 July 2007; published 10 September 2007)

We studied the nonequilibrium dynamics of the q-state Potts model in the square lattice, after a quench to subcritical temperatures. By means of a continuous time Monte Carlo algorithm (nonconserved order parameter dynamics) we analyzed the long term behavior of the energy and relaxation time for a wide range of quench temperatures and system sizes. For $q>4$ we found the existence of different dynamical regimes, according to quench temperature range. At low (but finite) temperatures and very long times the Lifshitz-Allen-Cahn domain growth behavior is interrupted with finite probability when the system gets stuck in highly symmetric nonequilibrium metastable states, which induce activation in the domain growth, in agreement with early predictions of Lifshitz [JETP **42**, 1354 (1962)]. Moreover, if the temperature is very low, the system always gets stuck at short times in highly disordered metastable states with finite lifetime, which have been recently identified as glassy states. The finite size scaling properties of the different relaxation times involved, as well as their temperature dependency, are analyzed in detail.

DOI: 10.1103/PhysRevE.76.031108 PACS number(s): 05.50.+q, 75.60.Ch, 75.10.Hk

I. INTRODUCTION

The problem of domain growth kinetics in systems with many degenerate ground states had attracted a lot of attention in the past [1–8]. In early works Lifshitz [1] and then Safran [2] posed the discussion about the effect of activated processes in the domain growth. They suggested that d-dimensional, q-state degenerate models could become trapped in local metastable states for $q \geqslant d+1$, which would then greatly slow down the relaxational kinetics. Their argument in two dimensions is that a honeycomb structure of hexagonal domains is stable under small distortions of the interfaces because such distortions do not increase the interfacial free energy. Large distortions due to fluctuations are then needed to move the interfaces and so domain growth becomes activated. The prototype of such a system is the q-state Potts model [9], whose Hamiltonian is given by

$$H = -J\sum_{nn} \delta(s_i,s_j), \quad J>0, \tag{1}$$

where $s_i=1,2,\ldots,q$, $\delta(s_i,s_j)$ is the Kronecker delta, and the sum runs over all the pairs of nearest-neighbor sites. Sahni and co-workers [3,4] performed Monte Carlo (MC) simulations with Glauber dynamics for values of q up to 64 in square and triangular lattices of size up to $N=200^2$ sites and time scales of the order 10^4 Monte Carlo steps (MCS) (1 MCS is defined as a complete cycle of N spin update trials, according to a Metropolis MC algorithm). On the square lattice they found evidence of metastable configurations composed by squares of different colors (i.e., different values of q) that freeze the dynamics a $T=0$; Viñals and Grant [5] obtained similar results in the square lattice. Moreover, they argue that those frozen configurations only effectively dominate at $T=0$ and growth at finite temperatures is not limited by activated processes [5]. Hence, for long enough times the average linear domain size should follow the Lifshitz-Allen-Cahn (LAC) law $l(t)\sim t^{1/2}$. This seems to be the case of the triangular lattice, where Grest and co-workers [6] reported results using MC simulations with $N=1000^2$ sites and values of q up to $q=64$ at very low temperatures, which are consistent with LAC behavior for any value of q, at least for time scales up to 10^4 MCS. Analytical results on a coarse grained model also confirm those results [8]. However, the time scales considered in those works are very short to exclude the existence of an activated process of the type predicted by Lifshitz [1] and Safran [2].

On the other hand, recent investigations [10–12] about the pinning configurations found in the square lattice [3–5] showed that the system gets stuck in those states at times scales longer than 10^4 MCS; pinning also happens at low but finite temperatures [13], although in that case the metastable states present a finite lifetime that increases with q [14]. Those works also showed that the nature of those highly disordered metastable states is more related to a glassy one [10–13] than to the type of configurations predicted by Lifshitz [1] and Safran [2]. We will refer hereafter to those disordered metastable states as the glassy ones.

In this work we concentrated mainly in the $q=9$ case in square lattices with $N=L\times L$ sites and periodic boundary conditions. Some complementary results are also presented for other values of q. The implementation of a continuous time MC algorithm or *n-fold* technique [15,16] allowed us to analyze a large statistics on system sizes up to $L=500$ and time scales running from 10^9 to 10^{14} MCS. Some details of the continuous time MC implementation are presented in Sec. II.

The main results of this work can be summarized as follows: after a quench from infinite temperature down to subcritical temperatures T, we found the existence of different relaxational regimes according to the quench temperature range. First of all there is some characteristic temperature $T^*<T_c$, such that for $T^*<T<T_c$ simple coarsening domi-

*ferrero@famaf.unc.edu.ar
†cannas@famaf.unc.edu.ar

nates the relaxation (that is, the domain growth follows the LAC law even for very long times), except very close to T_c, where evidence of nucleation relaxation mechanisms appear; however, the last case will not be analyzed in this work and the corresponding results will be presented in a forthcoming publication. For $T<T^*$ we found that, at long time scales (i.e., much longer than those considered in previous works), the LAC relaxation is interrupted when the system gets trapped in highly symmetric metastable states with finite probability (i.e., for a large fraction of realizations that do not decrease as the system size increases). We found two different types of those configurations: striped states and honeycomblike structures; the latter are configurations composed by macroscopic six-sided irregular polygonal domains of different colors. Striped states are composed by two macroscopic ferromagnetic domains with straight walls parallel to the coordinate axis and have been previously observed in the Ising model [17–21] ($q=2$) at $T=0$. For $q\geqslant 3$ and $T=0$ the probability to reach a striped state becomes zero in the thermodynamic limit [19]; we found that low but finite temperatures make that probability become finite. The presence of honeycomblike structures in the q-state Potts model is in agreement with the Lifshitz's prediction [1]. When the system reaches either striped or honeycomblike states the dynamics becomes activated.

Finally, we found a temperature $T_g \ll T_c$, such that for $T<T_g$ the system always gets stuck at intermediate times in a glassy state of the type reported previously [10–13] for other values of $q>4$. We found that for $q=9$ those states present a finite lifetime (i.e., independent of the system size) with a well-defined free energy barrier associated to it.

We also analyzed the scaling properties of the characteristic times associated with the different relaxation processes, as well as the probability of reaching a striped or honeycomb state for large values of q.

We verified that the whole relaxation scenario is qualitatively observed when open (instead of periodic) boundary conditions are used. All the numerical results are presented in Sec. III and some discussion is presented in Sec. IV.

Besides its theoretical interest, the large-q Potts model (or variations of it) is used for simulating the dynamics of a large variety of systems, such as soap froth [22,23], grain growth [24,25], and biological cells [26]. The present results help to establish the conditions under which equilibrium can be actually reached, as well as the different possible low temperature relaxation scenarios.

II. METHODS

We analyzed the time evolution under a type A dynamics (nonconserved order parameter) of the system described by Hamiltonian (1), after a quench from infinite temperature (i.e., a completely random initial configuration) down to subcritical temperatures. The Potts model undergoes a second order phase transition for $q=2$, 3, and 4 and a first order one for $q>4$, where the critical temperature in the square lattice is known exactly [27] for any value of q and is given by $T_c=1/\ln(1+\sqrt{q})$ (hereafter we will use natural units $k_B=J=1$). Most of our analysis was concentrated in the $q=9$ case, for which $T_c=0.721\,3\ldots$, and some complementary calculations were performed for $q=2$, 3, 4, 5, 15, and 30.

We were mainly interested in the late stages of the dynamics, where large domains are formed. In that case, the computational cost of a single spin flip dynamics (for instance, heat bath algorithm) becomes very high because the flipping probability of spins inside the domains (which are the majority) becomes very small. An efficient way to achieve longer time scales for reasonably large system sizes is the usage of *continuous time* MC methods or *n-fold* techniques [15]. In these types of algorithms a flip occurs at each step and the time such event would have elapsed in a single spin flip algorithm is calculated from the associated flipping probability. Let us briefly summarize the implementation of the algorithm for the nearest-neighbors q-state Potts model. For a given spin configuration we will call "potential spins" to the $q-1$ possible states for each site in the lattice, different from the present ones. All the potential spin of the system is then classified into lists, where members of a given list would produce the same change in the energy of the system, if chosen to replace the old spin state in the corresponding site. For a single flip there exist only nine possibilities $\left(\frac{\Delta E}{J}=-4,-3,-2,-1,0,1,2,3,4\right)$, so we have nine classes for any value of $q\geqslant 3$. In the Metropolis algorithm the probability of a potential spin belonging to the class l ($l=1,\ldots,9$) to be effectively flipped is

$$p_l=\frac{n_l}{N(q-1)}\min\left[1,\exp\left(-\frac{\Delta E_l}{k_BT}\right)\right], \tag{2}$$

where n_l is the number of spins in class l. The total probability of any flipping event occurring in a given step is

$$Q=\sum_l p_l. \tag{3}$$

In the present algorithm, at each step a class is sorted with probability (2) and a potential spin is sorted with equal probability among all the members in the class. After updating the corresponding spin and the lists, the time step is incremented by an amount

$$\Delta t=\frac{-\ln r}{NQ}, \tag{4}$$

where r is a random number uniformly distributed between zero and one and the time step Δt is measured in MCS. The details of the algorithm can be seen in Ref. [15]. The implementation of this algorithm allowed us to perform simulations for time scales running from 10^9 MCS (for sizes up to $L=500$) to 10^{14} MCS (for sizes up to $L=100$). In order to check the algorithm we also repeated several of the simulations using a single spin-flip algorithm (heat bath) for $L=200$ and time scales up to 10^6 MCS. The results were identical.

Our analysis of the dynamics was mainly focused on the behavior of two quantities: the average energy per spin $e(t)\equiv\langle H(t)\rangle/N$ as a function of t (the average was taken over different initial configurations and different realizations of the thermal noise) and the *equilibration time* τ, the last quantity was defined as the time at which the instantaneous en-

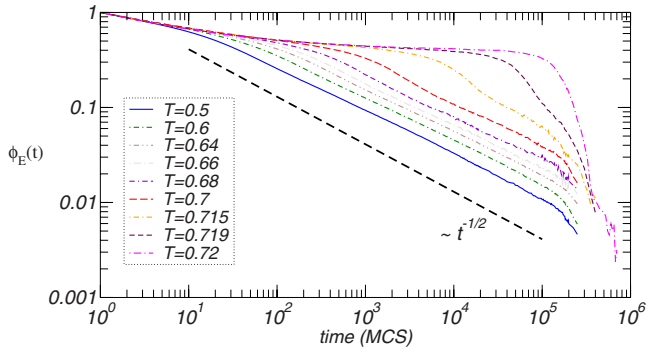

FIG. 1. (Color online) Relaxation function $\phi_E(t)$ for $L=300$ and $q=9$ and temperatures $T=0.5$ (bottom), 0.6, 0.64, 0.66, 0.68, 0.7, 0.715, 0.719, and 0.72 (top).

ergy falls below an equilibration threshold. Such a threshold was set as the equilibrium energy at the corresponding temperature plus one standard deviation, where those quantities were first calculated by running a set of simulations starting from the ordered state and letting the system equilibrate. We calculated the probability distribution (normalized histogram) $P(\tau)$ for different values of T and L.

III. RESULTS

In order to compare the behavior of the average energy per spin $e(t)=\langle H\rangle/N$ for different temperatures, we first introduce the relaxation function (or normalized excess of energy)

$$\phi_E(t) \equiv \frac{e(t)-e(\infty)}{e(0)-e(\infty)}, \tag{5}$$

where $e(\infty)$ is the equilibrium energy. In Fig. 1 we show the typical behavior of $\phi_E(t)$ for $L=300$ and temperatures between 0.72 and 0.5 ($T_c=0.721\,3\ldots$). For temperatures close enough to T_c ($0.715<T<T_c$) we see that the system clearly stuck in a high energy metastable state. Close examination of different quantities in the metastable state show that this corresponds to a disordered (i.e., paramagnetic) one and hence it is directly related to the first order nature of the transition. Moreover, we found evidence that in this regime relaxation is dominated by nucleation mechanisms, but the details of that analysis will be presented in a forthcoming publication. For temperatures $T<0.715$ we see that the metastable plateau disappears and the relaxation function decays (after a short transient) for all temperatures as $\phi_E(t)\sim t^{-1/2}$. Since the excess of energy with respect to the equilibrium state in a domain growth process is given by the average energy of the domain walls, a simple calculation shows that $\phi_E(t)\sim 1/l(t)$, $l(t)$ being the average linear domain size. Hence the behavior of Fig. 1 is consistent with the LAC law. As we will show later, the finite size scaling properties of the average typical equilibration time in this temperature range are also consistent with the LAC law.

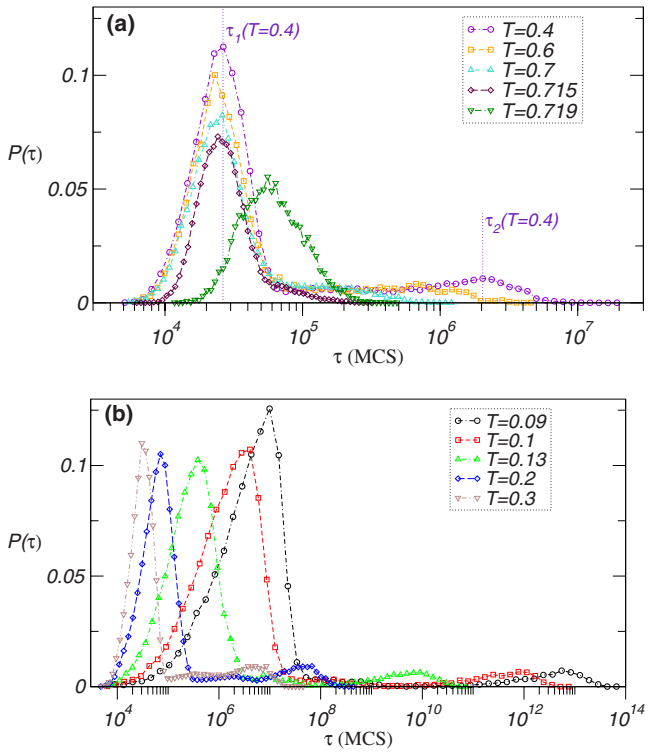

FIG. 2. (Color online) Equilibration time probability distribution $P(\tau)$ for $L=100$ and $q=9$. (a) Temperatures ranging from $T=0.4$ (top) to 0.719 (bottom). (b) Temperatures ranging from $T=0.3$ (left) to 0.09 (right).

A. Relaxation at intermediate temperatures and blocked states: Characterization and scaling

In Fig. 2 we see the typical behavior of $P(\tau)$ for an intermediate size ($L=100$) and different temperature ranges. The different dynamical regimes can be already appreciated in this figure. Close enough to T_c [$T=0.719$ in Fig. 2(a)] $P(\tau)$ exhibit a well-defined peak centered at a characteristic time $\tau_{nucl}\sim 10^5$ MCS, which is associated to a nucleation based relaxation mechanism already mentioned. As the temperature decreases below some temperature $0.715<T_n<T_c$, this peak is suddenly replaced by another one centered at a characteristic value τ_1, which is about one order of magnitude smaller than τ_{nucl} and remains almost independent of the temperature in the range $0.3<T<0.715$; in the temperature range $0<T\leqslant 0.2$ [see Fig. 2(b)], τ_1 exhibits a strong temperature dependency. For temperatures smaller than (but close to) T_n [see Fig. 2(a)], $P(\tau)$ develops a long right tail; for temperatures $T<T^*\approx 0.6$ the tail becomes a distinct peak centered at a new characteristic time τ_2, which increases exponentially as the temperature decreases. This behavior indicates the existence of two distinct phenomena affecting the relaxation at different time scales, where T^* acts as a reference temperature signaling the time scales separation crossover point. The temperature behavior of τ_1 and τ_2 is summarized in the Arrhenius plot of Fig. 3.

We will show that τ_1 is associated with simple coarsening processes that follow LAC law for all times, while τ_2 is associated to processes in which the system gets stuck in

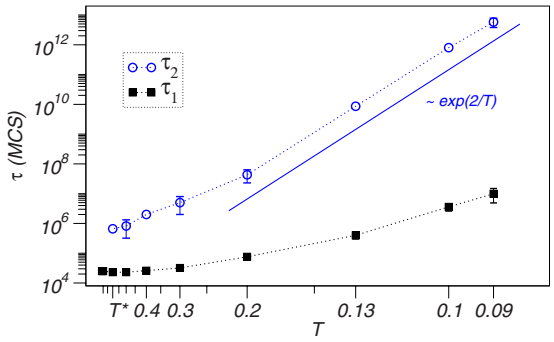

FIG. 3. (Color online) Characteristic relaxation times τ_1 and τ_2 vs $1/T$ for $L=100$ and $q=9$; the same qualitative behaviors are observed for other system sizes. The continuous lines are a guide to the eye.

striped metastable states, composed by two ferromagnetic states whose walls are parallel to coordinate axis, as shown in the example of Fig. 4. Those types of metastable states have been already observed in the two-dimensional Ising model ($q=2$) at zero temperature, where they become frozen [17–21]. At finite temperature, striped states perform a random parallel movement in the direction perpendicular to the walls. Hence in a finite system those states relax to equilibrium when both walls collapse. Spirin, Kaprivsky, and Redner [18] showed that the basic mechanism for the parallel movement of a straight domain wall is the creation of a "dent," that is, the flip of one of the spins adjacent to the wall. Since after flipping the spin its neighbors can flip without energy cost, the energy barrier for the creation of a dent is 2 (in units of the coupling constant J) for the $q=2$ Potts model (or 4 for the Ising model). For $q>2$ the energy cost of any other movement (including a flipping to a third color different from those of the domains) is larger. Hence once the striped state is reached, the time needed to relax should be basically independent of q and this is consistent with the Arrhenius behavior $\tau_2 \sim e^{2/T}$ observed in Fig. 3.

From Fig. 3 we can notice also that, for a wide range of temperatures $T<T_n$ (approximately down to $T\approx 0.2$) τ_1 remains almost independent of T, consistently with a simple

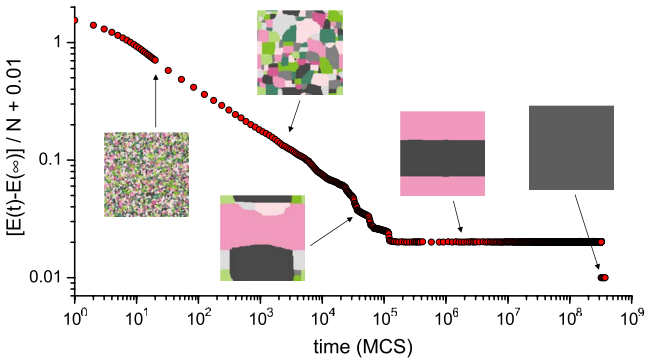

FIG. 4. (Color online) Energy per spin as a function of time and typical spin configurations in one realization of the stochastic noise, when the system gets stuck in a striped configuration ($L=200$, $q=9$, and $T=0.2$). The different colors codify different spin values $s_i=1,\ldots,9$.

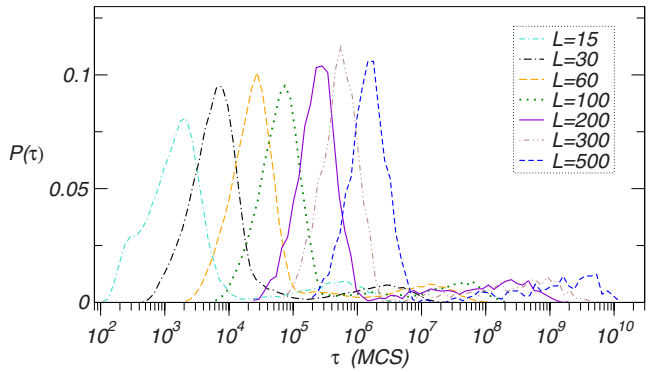

FIG. 5. (Color online) Equilibration time probability distribution $P(\tau)$ for $T=0.2$ and $q=9$ and system sizes ranging from $L=15$ (left) to 500 (right).

coarsening behavior; at lower temperatures we see a crossover into an activated behavior that will be analyzed later.

A deeper understanding of the mechanisms involved in the relaxation can be obtained from the finite size scaling of the different quantities involved. In Fig. 5 we show the typical behavior of $P(\tau)$ for different system sizes at a fixed temperature $T=0.2$. The first thing we note is that the two-peak structure remains in the large L limit. Moreover, the ratio between the areas below both peaks becomes constant in such a limit. The same property is observed for temperatures up to T^*. We will analyze this in more detail at the end of this section. Let us now consider the finite size scaling of the relaxation times.

From Fig. 6 we see that $\tau_1 \sim L^2$ for a wide range of temperatures, both above and below T^*. This is also consistent with a simple coarsening process, in which equilibration will be attained once $l(\tau) \sim \tau^{1/2} \sim L$.

Let us now analyze the finite size scaling of τ_2. Spirin, Kaprivsky, and Redner [18] suggested that, at low enough temperatures, the movement of a flat interface will be dominated by processes involving a single dent creation; once the dent is created it performs a random walk, until either the dent disappears or it covers the whole line, where the typical time needed for the last event scales as [18] L. This mechanism leads to a random walk movement of both interfaces, so there must be typically L^2 such hopping events for the inter-

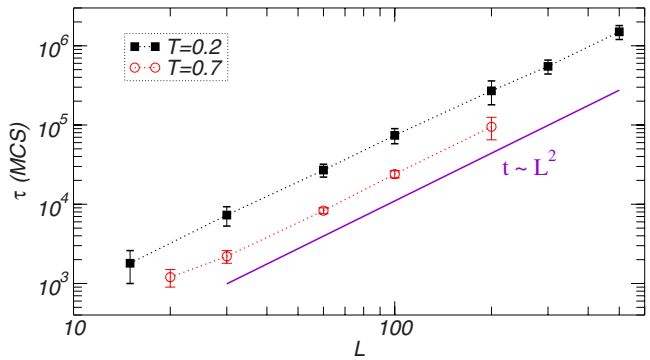

FIG. 6. (Color online) Characteristic relaxation time τ_1 vs L for $q=9$ and different temperatures; dotted lines are a guide to the eye.

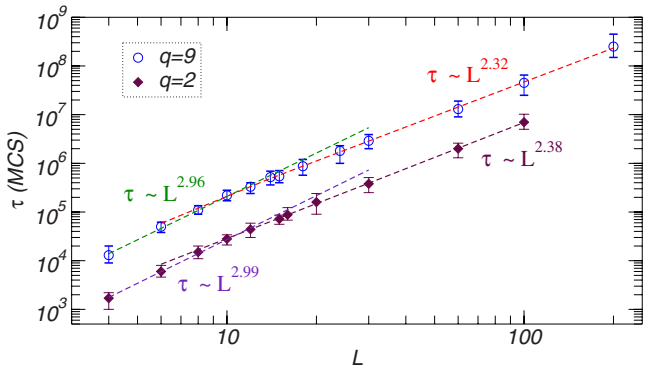

FIG. 7. (Color online) Characteristic relaxation time τ_2 vs L for $T=0.2$ and different values of q. The dashed lines correspond to linear fittings.

faces to meet and therefore the relaxation time should scale as [18] L^3. However, this argument only works for small system sizes. Once a dent is created, the probability of the creation of new dents along the interface, before the dent covers the line, increases with the system size; therefore the typical time for a one-site hoping event of an entire interface should increase slower than linearly with L and τ_2 slower than L^3. This can be appreciated in the clear crossover from $\tau_2 \sim L^3$ to $\tau_2 \sim L^\omega$ with $\omega < 3$ around $L=15$, observed in Fig. 7, both for $q=2$ and 9 (the same effect is observed for any temperature $T \leqslant 0.2$). Striped states appear for temperatures up to T^*, but the walls movements are no longer dominated by one-site hopping events for $T > 0.2$; instead of that, a direct inspection of the spin configuration during relaxation shows that, at temperatures close to T^* the movements of the domain walls resemble (for large system sizes) that of elastic lines subjected to a random noise. Hence the temperature dependence of τ_2 departs from the $e^{2/T}$ behavior, as can be seen from Fig. 3. However, the finite size scaling $\tau_2 \sim L^\omega$ still holds for temperatures up to T^*, where the exponent ω displays a marked increase with the temperature, reaching values slightly larger than 3 as T approaches T^* (see Fig. 8). Those values of the exponent can be understood through the following argument. Suppose that each line behaves as a chain of L unit masses joined by springs, constrained to move along the direction perpendicular to the wall and sub-

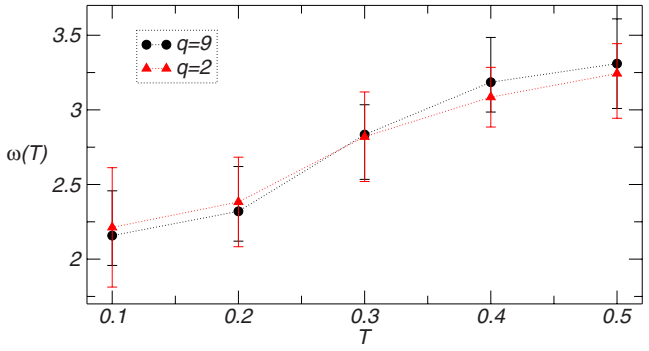

FIG. 8. (Color online) Finite size scaling exponent ω of the characteristic relaxation time τ_2 as a function of T for different values of q; dotted lines are a guide to the eye.

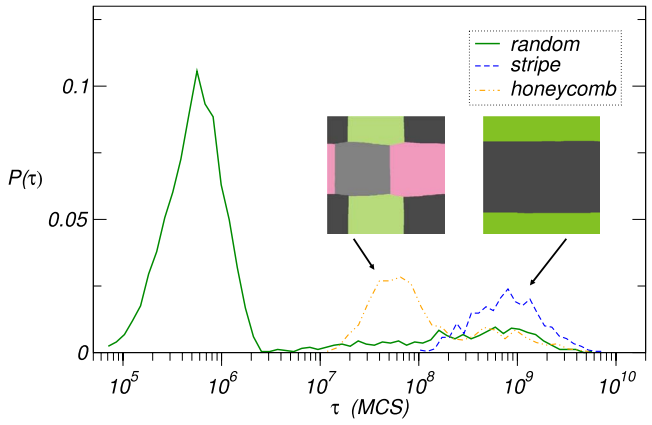

FIG. 9. (Color online) Equilibration time probability distribution $P(\tau)$ starting from different initial configurations (arbitrary normalization) for $L=300$ and $T=0.2$. The inset images show typical blocked spin configurations at the corresponding times.

jected to independent white noise. By solving the corresponding Langevin equations in the overdamped limit, a simple calculation shows that the distance between the centers of mass of both chains performs a Brownian motion with an effective diffusion coefficient that scales as $D \sim L^{-1}$. Since the distance between walls is of the order of L, this implies that the typical time needed for the walls to join each other should scale approximately as L^3. For $q=2$ Lipowski [17] has shown that this scaling holds even for relatively large values of the temperature $T/T_c(2) \approx 0.8$. The results of Fig. 8 suggest that the scaling properties of τ_2 are independent of q, showing that large degeneracies in the ground state have no influence in this relaxation process.

Let us return to the equilibration time probability distribution $P(\tau)$. Another salient feature of this distribution for temperatures $T < T^*$ is that the right peak broadens for large system sizes. To show this we redraw $P(\tau)$ for $L=300$ and $T=0.2$ in Fig. 9 (full line). A careful inspection of individual processes shows that such a broad peak is actually associated with two different types of metastable configurations: the striped ones already described and honeycomblike structures; the latter are composed macroscopic six-sided irregular polygonal domains of different colors (see inset of Fig. 9), where the angles between domain walls at the threefold edges fluctuate around 120°. Those states are in agreement with the Lifshitz prediction [1] for $q \geqslant 3$ and we shall call them Lifshitz states. By a calculation of the equilibration time starting directly from the Lifshitz and striped states, we verified that the broad peak of $P(\tau)$ is actually a superposition of two peaks, each one with its own distinctive maximum at characteristic times τ_2, for the striped states, and τ_3 for the Lifshitz ones (see Fig. 9). Lifshitz states are only detectable for system sizes $L \geqslant 100$. Actually, an isolated threefold vertex between flat domain walls of the type predicted by Lifshitz [1] also appears for smaller system sizes, but complete honeycomblike structures can be stabilized during detectable time scales (i.e., larger than the characteristic coarsening time scales) only for large enough system sizes. To determine the scaling properties of τ_3, we calculated the

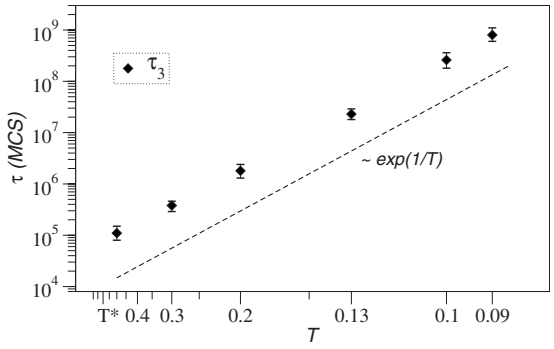

FIG. 10. Characteristic relaxation time τ_3 vs temperature for $q=9$ and $L=100$; the continuous line is a guide to the eye.

escape time probability distribution starting from the closest configuration to a Lifshitz state, that is, from an almost perfect four-colored honeycomb configuration (commensurability with the system size does not always allow a perfect honeycomb structure) for different values of L and T; we show an example in Fig. 9. We verified that the system quickly relaxes from that configuration into a Lifshitz state, from which it can either relax directly to the equilibrium state or pass first to a striped state, giving rise to a second peak in the corresponding probability distribution (see Fig. 9). For completeness, we also calculated the escape time probability distribution starting from a perfect two-domains striped state; the result is also shown in Fig. 9.

The temperature dependency of τ_3 is shown in Fig. 10, where we see that it displays a clear Arrhenius behavior with an activation barrier of height one, which is the minimum possible energy barrier associated with a single spin flip. This can be understood if we analyze the basic mechanisms behind the relaxation from Lifshitz states. We observed that Lifshitz states relax when two vertices of a hexagon edge collapse. A vertex movement, with the consequent displacement of the converging walls, occurs through a series of random hopping events. In Fig. 11 we show an example of the hopping of a vertex one site to the right; one-site hopping events in the other directions follow a similar process with the same energy cost. The movement of a vertex starts with the creation of a dent, by flipping one of the spins located at the neighbor sites of the vertex, as depicted in Fig. 11(b). This movement has an energy cost of one unit. Once the dent is created, the neighbor spins at the three converging walls are free to flip without energy cost [see Figs. 11(c) and 11(d)], generating a diffusive motion of the dent along the three lines, and may lead to the displacement of the whole lines. This hopping movement of the vertex ultimately leads to the collapse of two of them and the consequent disappearance of the Lifshitz state. The whole mechanism is completely similar to that described by Spirin, Kaprivsky, and Redner [18] in the case of a flat wall between two striped domains, except that the creation of a dent adjacent to a vertex has an energy cost of just one energy unit (instead of 2, as in the case of a dent in a flat interface), which explains the behavior of Fig. 10. Since hexagonal domains in a Lifshitz state are macroscopic, the same finite size scaling arguments used by Spirin, Kaprivsky, and Redner [18] for the

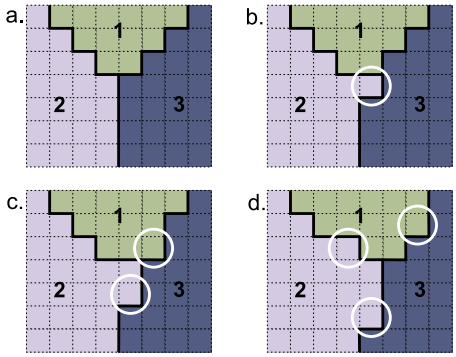

FIG. 11. (Color online) Basic relaxation mechanism of a Lifshitz state at low temperatures. The circle in (b) marks the creation of a dent in the vertex of (a), by flipping a spin from $2\rightarrow 3$ with an energy cost $\Delta E=1$. Circles in (c) and (d) exemplify spins that can flip without energy cost ($\Delta E=0$) along the three converging walls. The whole process may lead to the hopping of the whole structure (vertex plus walls) and ultimately to the collapse of two vertices.

relaxation time apply in this case. Hence, one expects $\tau_3 \sim L^{\omega} e^{1/T}$. For the system sizes available, we verified this scaling at low temperatures with an exponent $\omega \approx 3$, but we would expect this value to be reduced for larger system sizes, as in the case of striped states (τ_2).

B. Probability of blocked states

We analyzed the probability $P_b(q)$ of getting stuck in a blocked state. We defined blocked states as those characterized by flat walls between domains. For $q \geqslant 3$ this includes Lifshitz and striped states. For $q=2$ the system can also get trapped in another type of blocked states, characterized by diagonal stripes, whose interfaces fluctuate without energy cost [19]; we shall call them diagonal states. For $q \geqslant 3$ we did not observed diagonal states at finite temperatures. Although their presence for $q \geqslant 3$ with low probability cannot be excluded, probably they are replaced at finite temperature by the Lifshitz states.

From the previous calculations of $P(\tau)$ we could estimate $P_b(q)$ by defining for (for every value of T and L) a threshold value $\tau_t(T,L)$, such that a single realization with $\tau > \tau_t$ is attributed to the presence of a blocked state; τ_t can be estimated as the first minimum of $P(\tau)$ located above τ_1 (see, for instance, Fig. 5). This procedure reduces the calculation of $P_b(q)$ to a binomial experiment. Hence a simple calculation shows that a sample size of 2000 runs is enough to guarantee a statistical error smaller than 1% in all cases, thus saving a lot of CPU time.

In Fig. 12 we show the results for $q=9$. The main source of error in this calculation is the choice of τ_t, which is not always evident, due to large fluctuations in the histograms for small sizes and very low temperatures; the error bars in Fig. 12 were estimated by varying τ_t. From Fig. 12(a) we see that, at $T>0$, $P_b(9)$ saturates in a finite value for $L \geqslant 100$, indicating a finite probability in the limit $L \rightarrow \infty$. In Fig. 12(b) we show the temperature dependency of the saturation value. We see that $P_b(9)$ goes to zero as $T \rightarrow 0$, consistent with the

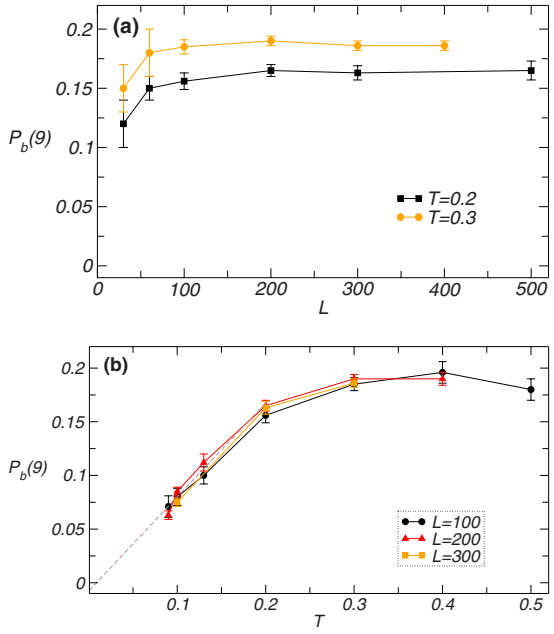

FIG. 12. (Color online) Probability of getting stuck in a blocked state $P_b(q)$ for $q=9$: (a) as a function of L for different temperatures and (b) as a function of T for different sizes. The dashed line corresponds to a linear fitting of the points for $L=200$, giving an extrapolated value of 0.008 ± 0.01 at $T=0$.

results of Spirin, Kaprivsky, and Redner [19].

Next we analyzed the probability $P_b(q)$ as a function of q. The results are shown in Fig. 13 for $T=0.15$ and values of q ranging from $q=2$ up to $q=30$. For $q=2$ and $T=0$ the probability of reaching a striped state is [18,28] 1/3, while the probability of reaching a diagonal state is [19] ≈ 0.04. At $T=0.15$ we found the values ≈ 0.345 and ≈ 0.045, respectively, giving rise to the value $P_b(2)\approx 0.39$. The differences with the $T=0$ values are consistent with the enhancement of the probability at finite temperature, already observed for $q=9$.

For $q \geqslant 3$ the probability $P_b(q)$ falls down to a temperature dependent finite value, that is almost independent of q and smaller than half of $P_b(2)$.

It is worth noting that Spirin, Kaprivsky, and Redner [19] reported another type of blocked states for $q=3$, characterized by both straight walls and diagonal walls, the latter fluctuating without energy cost; they call these states "blinkers." We did not observe blinkers at finite temperature, at least for periodic boundary conditions. Although their existence with low probability cannot be excluded, probably they decay into Lifshitz states in time scales smaller than the characteristic Lifshitz relaxation times.

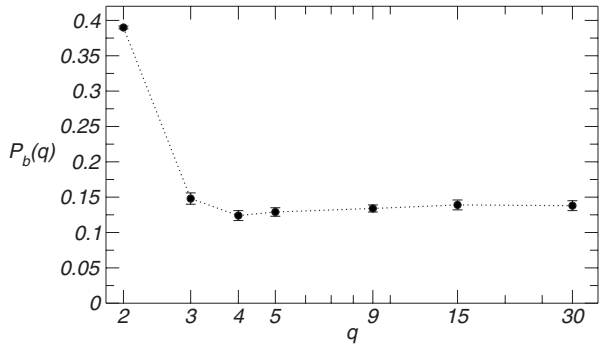

FIG. 13. Probability of getting stuck in a blocked state $P_b(q)$ for $L=200$ and $T=0.15$.

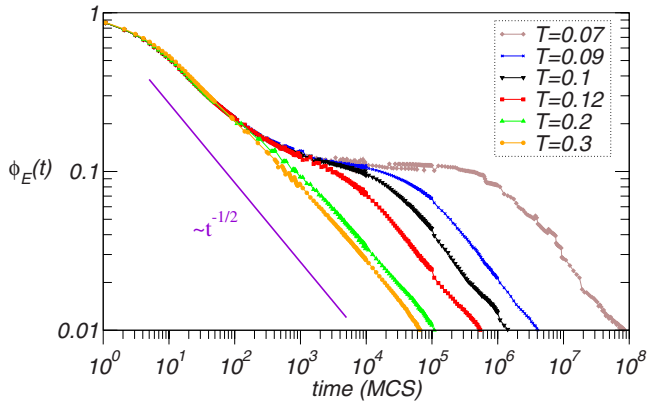

FIG. 14. (Color online) Relaxation function for $q=9$, $L=200$, and temperatures 0.3 (left), 0.2, 0.12, 0.1, 0.09, and 0.07 (right).

C. Low temperatures relaxation: Glassy states

Let us now analyze the coarsening at very low temperatures. The increase of τ_1 for temperatures $T<0.2$ observed in Fig. 3 indicates that the normal coarsening is affected by some kind of activated process. The increase in this relaxation time is associated with the plateau displayed by the relaxation function in Fig. 14. We found that this plateau appears below some characteristic temperature $0.1<T_g<0.2$ for $q=9$. This plateau corresponds to a disordered metastable state characterized by almost square-shaped domains with a wide distribution of sizes (see inset in Fig. 15). That type of metastable state was previously reported for $q=7$ and it was identified as a glassy one [10–12]. These states are only present for [13] $q>4$. We verified that for $q=9$ the

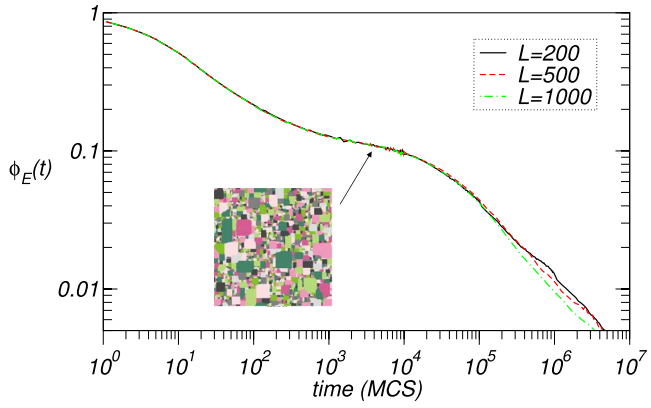

FIG. 15. (Color online) Relaxation function for $q=9$, $T=0.1$, and different values of L. The inset shows a typical configuration of the glassy state associated with the plateau.

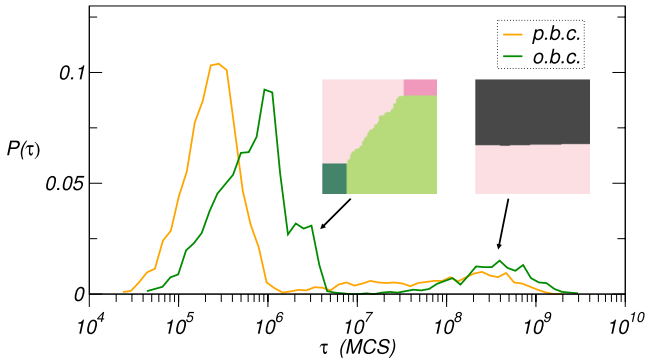

FIG. 16. (Color online) Equilibration time probability distribution $P(\tau)$ for $q=9$, $L=200$, and $T=0.2$, using periodic (p.b.c) and open (o.b.c) boundary conditions. The inset images show typical blocked spin configurations observed with o.p.c.

normal coarsening is always interrupted for $T<T_g$ and the system gets stuck in one of those glassy states, from which it relaxes through a complex sequence of activated jumps. This explains the exponential increase of τ_1 observed in Fig. 3 for $T<0.2$. Once the system relaxes from the glassy state, it can be either directly equilibrate or decay first in a blocked state.

In Fig. 15 we show the typical behavior of a relaxation function for $q=9$ at a fixed temperature $T<T_g$ and different system sizes. We see that the relaxation time (τ_1) is size independent for $L>200$, which shows that the lifetime of the glassy states remains finite in the thermodynamic limit.

D. Boundary conditions

Finally, we analyzed the influence of the boundary conditions in the relaxation. To this end, we repeated some of the previous calculations using open boundary conditions. We found that the overall relaxation scenario found using periodic boundary conditions repeats qualitatively for open ones. Moreover, the relaxation time associated with striped configurations appears to be of the same order of magnitude of that corresponding to periodic boundary conditions. Although a more systematic study should be done to confirm that, it seems reasonable since the basic activated mechanisms here described should be still dominant in the case of open boundary conditions. In Fig. 16 we show an example of the equilibration time probability distribution for $q=9$ and some typical blocked spin configurations. In this case, Lifshitz states are no longer composed only by hexagons for relatively small system sizes (due to the presence of the borders), but we see clearly the presence of a stable three-colored vertex. Indeed, the observed configurations strongly resemble the blinking states reported in Ref. [19].

IV. SUMMARY AND CONCLUSIONS

The main conclusions of this work are summarized in the scheme of Fig. 17. After a quench from infinite temperature down to subcritical temperatures, the Potts model with single spin flip kinetics and periodic boundary conditions presents for $q>4$ different relaxational regimes, determined by different crossover characteristic temperatures. Close enough to the critical temperature, i.e., for $T_n<T<T_c$, relaxation is dominated by nucleation mechanisms. For intermediate temperatures $T^*<T<T_n$ the system crosses over into a simple coarsening dominated regime where LAC law $l(t)\sim t^{1/2}$ holds until full equilibration, for most of the realizations of the stochastic noise. For lower temperatures $T_g<T<T^*$ the normal coarsening process is interrupted when the system gets stuck into highly symmetric blocked configurations, composed by macroscopic ferromagnetic domains, namely, striped and Lifshitz states. In those cases, the dynamic becomes activated with characteristic energy barriers, which give rise to distinct time scales for the different process.

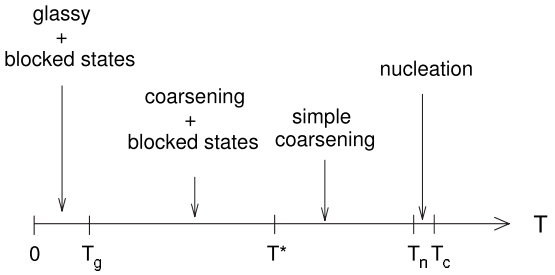

FIG. 17. Dynamical regimes in the long term relaxation of the q-state Potts model with $q>4$, after a quench from infinite temperatures down to a subcritical temperature T.

Concerning the role of temperature in the relaxation through blocked states, we found that it has a double effect: at short time scales it enhances the probability of reaching them (which is zero at $T=0$) and at long time scales it allows escape from them through activation. At least for $q=9$, our simulations (for system sizes up to $L=500$) suggest that the probability of reaching a blocked state at finite temperatures remains finite when $L\to\infty$.

Striped states were previously found and characterized for the Ising model ($q=2$) at very low temperatures. We found that their influence in the relaxation process is relevant for any value of q, even at relatively large values of T, but their occurrence probability is smaller for $q\geqslant 3$ than in the Ising case.

We found that the relaxation times associated with the blocked states present in general the finite size scaling behavior $\tau\sim L^{\omega}$, where the exponent ω depends on T, taking values between 2 and 4. Such values of the exponent make the associated time scales several orders of magnitude larger than those associated with a normal coarsening process (which scale as L^2) for large enough sizes, even at relatively large values of the temperature.

Lifshitz predictions have been recently verified in the phase separation dynamics of diblock copolymers (Cahn-Hillard model), in a two-dimensional hexagonal substrate [29]. We verified that the Lifshitz prediction also holds for the q state Potts model with $q\geqslant 3$, even in a square lattice, if the system size is large enough. This strong finite size effect is probably due to the square symmetry of the lattice (large system sizes are required in order for the influence of the lattice to be faded out) and one should expect it to be re-

duced in a lattice with threefold symmetry (for instance, triangular).

At very low temperatures $T<T_g$ the system always gets trapped in glassylike metastable configurations whose lifetime is size-independent and diverges for $T\to\infty$. After relaxation from the glassy state, the system can again get trapped in a blocked state. Even when the glassy states do not dominate the relaxation at long enough time scales, a complete description of the relaxation dynamics cannot exclude their existence and therefore they deserve further investigations. Finally, we verified that the whole qualitative relaxation scenario appears both for periodic and open boundary conditions, although the finite size scaling of the relaxation times may differ in both cases.

ACKNOWLEDGMENTS

Fruitful discussions with M. Ibañez de Berganza, F. A. Tamarit, and C. B. Budde are acknowledged. This work was partially supported by grants from CONICET (Argentina), SeCyT, Universidad Nacional de Córdoba (Argentina), FONCyT Grant No. PICT-2005 33305 (Argentina), and ICTP Grant No. NET-61 (Italy).

[1] I. Lifshitz, Sov. Phys. JETP **15**, 939 (1962).
[2] S. A. Safran, Phys. Rev. Lett. **46**, 1581 (1981).
[3] P. S. Sahni, D. J. Srolovitz, G. S. Grest, M. P. Anderson, and S. A. Safran, Phys. Rev. B **28**, 2705 (1983).
[4] M. P. Anderson, D. J. Srolovitz, G. S. Grest, and P. S. Sahni, Acta Metall. **32**, 783 (1984).
[5] J. Vinals and M. Grant, Phys. Rev. B **36**, 7036 (1987).
[6] G. S. Grest, M. P. Anderson, and D. J. Srolovitz, Phys. Rev. B **38**, 4752 (1988).
[7] S. Kumar, J. D. Gunton, and K. K. Kaski, Phys. Rev. B **35**, 8517 (1987).
[8] C. Sire and S. N. Majumdar, Phys. Rev. Lett. **74**, 4321 (1995).
[9] F. Y. Wu, Rev. Mod. Phys. **54**, 235 (1982).
[10] A. Petri, Braz. J. Phys. **33**, 521 (2003).
[11] M. de Oliveira, A. Petri, and T. Tomé, Physica A **342**, 97 (2004).
[12] M. Oliveira, A. Petri, and T. Tomé, Europhys. Lett. **65**, 20 (2004).
[13] M. I. de Ibañez, V. Loretto, and A. Petri, Philos. Mag. **87**, 779 (2007).
[14] M. I. de Ibañez, E. E. Ferrero, S. A. Cannas, V. Loretto, and A. Petri, Eur. Phys. J. Special Topics **143**, 273 (2007).
[15] A. B. Bortz, M. H. Kalos, and J. L. Lebowitz, J. Comput. Phys. **17**, 10 (1975).
[16] M. A. Novotny, Phys. Rev. Lett. **74**, 1 (1995).
[17] A. Lipowski, Physica A **268**, 6 (1999).
[18] V. Spirin, P. L. Krapivsky, and S. Redner, Phys. Rev. E **63**, 036118 (2001).
[19] V. Spirin, P. L. Krapivsky, and S. Redner, Phys. Rev. E **65**, 016119 (2001).
[20] P. Sundaramurthy and D. L. Stein, J. Phys. A **38**, 349 (2005).
[21] P. M. C. de Oliveira, C. M. Newman, V. Sidoravicious, and D. L. Stein, J. Phys. A **39**, 6841 (2006).
[22] J. A. Glazier, M. P. Anderson, and G. S. Grest, Philos. Mag. B **62**, 615 (1990).
[23] J. A. Glazier and D. Weaire, J. Phys.: Condens. Matter **4**, 1867 (1992).
[24] D. Weaire and J. A. Glazier, Mater. Sci. Forum **94-96**, 27 (1992).
[25] G. L. Thomas, R. M. C. de Almeida, and F. Graner, Phys. Rev. E **74**, 021407 (2006).
[26] F. Graner and J. A. Glazier, Phys. Rev. Lett. **69**, 2013 (1992).
[27] T. Kihara, Y. Midzuno, and T. Shizume, J. Phys. Soc. Jpn. **9**, 681 (1954).
[28] M. Fialkowski and R. Holyst, Eur. Phys. J. E **16**, 247 (2005).
[29] L. R. Gomez, E. M. Valles, and D. A. Vega, Phys. Rev. Lett. **97**, 188302 (2006).